M.S. THESIS

DEVELOPMENT OF MASS FABRICATION METHOD TO ENCODED MAGNETIC BEADS FOR MULTIPLEXED BIOASSAYS

다중화 바이오 어세이를 위한 코드화된 자성 입자 양산 방법 개발

BY

HUNJONG NA

AUGUST 2013

DEPARTMENT OF ELECTRICAL ENGINEERING AND COMPUTER SCIENCE
COLLEGE OF ENGINEERING
SEOUL NATIONAL UNIVERSITY

M.S. THESIS

DEVELOPMENT OF MASS FABRICATION METHOD TO ENCODED MAGNETIC BEADS FOR MULTIPLEXED BIOASSAYS

다중화 바이오 어세이를 위한 코드화된 자성 입자 양산 방법 개발

BY

HUNJONG NA

AUGUST 2013

DEPARTMENT OF ELECTRICAL ENGINEERING AND COMPUTER SCIENCE
COLLEGE OF ENGINEERING
SEOUL NATIONAL UNIVERSITY

DEVELOPMENT OF MASS FABRICATION METHOD TO ENCODED MAGNETIC BEADS FOR MULTIPLEXED BIOASSAYS

다중화 바이오 어세이를 위한 코드화된 자성 입자 양산 방법 개발

지도교수 권 성 훈

이 논문을 공학석사 학위논문으로 제출함

2013 년 5 월

서울대학교 대학원

전기컴퓨터 공학부

나 훈 종

나훈종의 공학석사 학위논문을 인준함

2013 년 8 월

위 원 장 : 박 영 준

부위원장 : 권 성 훈

위 원 : 서 종 모

Abstract

DEVELOPMENT OF MASS FABRICATION METHOD TO ENCODED MAGNETIC BEADS FOR MULTIPLEXED BIOASSAYS

HUNJONG NA

DEPARTMENT OF ELECTRICAL ENGINEERING AND COMPUTER SCIENCE

COLLEGE OF ENGINEERING

SEOUL NATIONAL UNIVERSITY

With the arrival of multiplexed assay technologies, researchers have gained access to large amounts of information by allowing a sample to react with diverse probe molecules. The multiplex assays reduce the amount of reagents, handling time and complex laborious experimental procedures. An encoded suspension array using micro-beads enables easy handling of various molecules and simultaneous measures the multiple targets in each sample. In our lab, we have developed the encoded micro-beads for multiplexed assays and succeeded

to perform DNA genotyping assay, Elisa assay, elispot assay, western blot and so on. However, improvements still remain to achieve more reliable and reproducible assay. Firstly, the number of beads fabricated in lithography step has to be increased to acquire sufficient population of data. Secondly, variations among the beads which occurred in lithography step and surface modification step have to be decreased.

This thesis presents the improvised process to address the aforementioned improvements. The process is broadly discussed in two steps: 1) synthesis of magnetic nanoparticles. The incorporation of magnetic nanoparticles into the beads not only increased the convenience in handling, but also reduced the variations which occurred in surface modification step. 2) The development of a mass fabrication method for encoded beads which does not require realignment at each operation and, therefore, reduced variations which occurred in lithography step. Finally, improved assay results by reducing variations will be showed.

Keywords: Multiplexed assay, Bioassays, Encoded beads, Mass fabrication, Magnetic nanoparticles, Superparamagnetic

Student Number: 2011-20827

Publications in Conference Proceedings

International Conference

- Y. Jung, **H. Na**, J. Choi, and S. Kwon, "Inventing and Developing a Multi-functional Microplate System for Antibiotic Susceptibility Test Using Single Cell Growth Tracking", The 1st Society for Laboratory Automation and Screening, San Diego, USA, February 2012. (Poster)

- Y. Jung, J. Choi, **H. Na**, J. Kim, and S. Kwon, "Rapid Antibiotic Susceptibility Test in the Agarose Microfluidic Channel", The 1st Society for Laboratory Automation and Screening, San Diego, USA, February 2012. (Poster)

Domestic Conference

- **H. Na**, Y. Jung, J. Choi, and S. Kwon, "Multi-functional Novel Agar Plate System for Observing Bacterial Single Cell : Slip™ System", 2012 International Meeting of the Microbiological Society of Korea, Seoul, Korea, May 2012. (Poster)

- Y. Jung, **H. Na**, J. Choi, and S. Kwon, "The Multi-functional Microplate System for Antibiotic Susceptibility Test using Single Cell Growth Tracking", The Korean Biochip Society 2011 Autumn Conference, Ulsan, Korea, November 2011. (Poster)

- **H. Na**, J. Koh, E. Kim, W. Park, and S. Kwon, "Microfluidic Channel Prototyping using Programmable LCD Photomask", The 13th Korean MEMS Conference, Jeju, Korea, April 2011. (Poster)

Contents

List of Figures

Chapter 1

Introduction

The multiplexed assay technologies have been used in biological and medical studies on gene profiling, drug screening, and clinical diagnostics. Researchers obtain large amounts of information by allowing a sample to react with diverse probe molecules. By multiplexing, we can dramatically increase the amount of useful information from rare or volume-limited samples. Moreover multiplexed assays reduce reagent handling, cost of reagents, laborious works and time. An encoded suspension array has developed as a high-throughput, convenient, and low-cost method. Encoded micro-beads with probe molecules that react with a sample are selectively observed with their codes, enabling researchers to easily determine the content of the sample. These beads enable easy handling of various molecules and simultaneous measurement of multiple targets in each sample. Bead based

multiplexed assays for quantitation and detection of soluble proteins and intracellular markers have attracted considerable attention from biological and medical researchers [1].

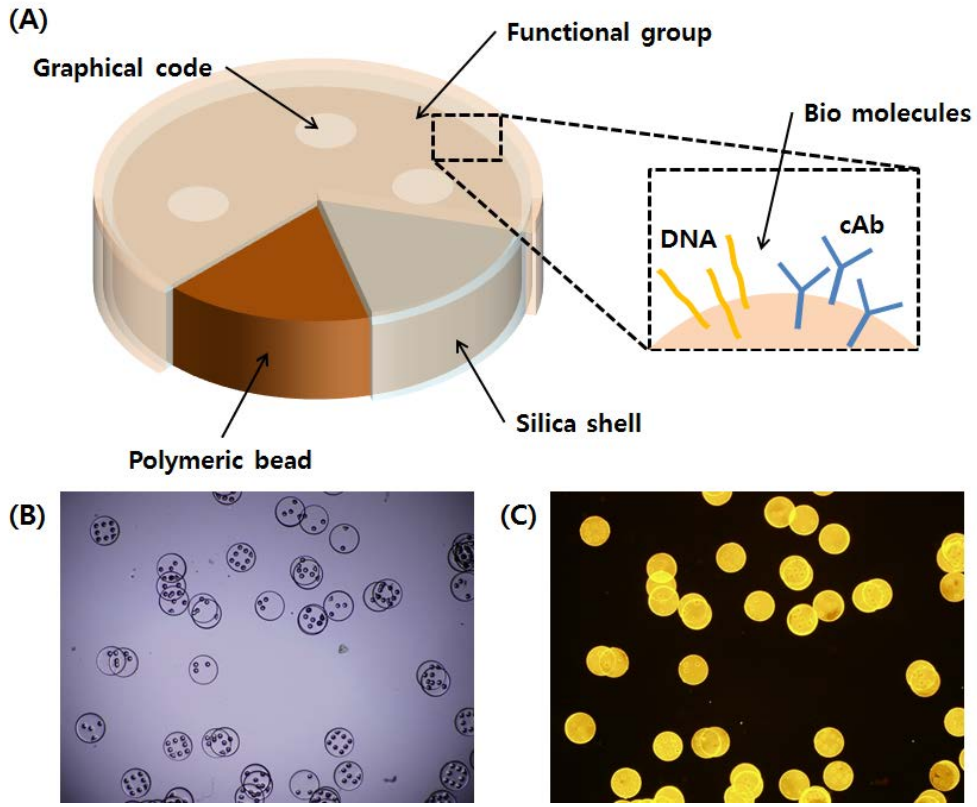

Figure 1 (A) The structure of an encoded micro-bead for multiplexed bioassays. (B) Bright field and (C) fluorescence images of multiplexed DNA hybridization assay.

The structure of encoded micro-beads for multiplexed bioassays which have developed in our laboratory is shown in figure 1 (A). At first, we produced encoded polymeric micro-beads by using a UV curable resin and these beads were

easy to make various shapes. These encoded polymeric beads were fabricated by performing optofluidic maskless lithography (OFML) [2]. The size and shape of each bead could be individually controlled by modifying the mask design, magnification, and intensity of UV. Two-dimensional graphical codes could be encoded during bead fabrication step [3]. The resultant coded polymer beads were followed by silica coating (will be publish). Silica coating not only gives chemical and mechanical stability to the beads but also enables to directly adopt well-established silica surface chemistry such as introduction of carboxyl or amine groups which can form covalent bond with various biomolecules [4, 5]. Using bead based assay system, we have performed various multiplexed bioassay such as HPV genotyping, cytokine Elisa, western blot, elispot and so on.

Although it is possible to perform multiplexed bioassay with our beads, improvements are needed to acquire more reliable and reproducible data. First, OFML system has the advantage of a variety of conditions can be test, but the number of beads that can be produced is limited because it requires one UV injection to produce one bead and, therefore. Also, to produce sufficient number of beads, we have to operate the system many times and have to re-align the optic system at each operation. In such a system is bound to cause variation among the beads in the lithography process. Above all, the lack of the sample population and the variation among the beads decline reliability of assay results. Second, the beads

handling is inconvenient because it does not contain magnetic materials yet. This causes not only inconvenience but also variation among the beads during surface treatment step because it is impossible to solution exchange completely.

To solve these problems, we developed mass fabrication method for encoded micro-beads which does not require realignment at each operation. Additionally, by introducing magnetic nanoparticles into the micro-beads, convenience and reduced variation is obtained. Therefore, the encoded magnetic beads provide fast and accurate data in bioassay. Here, I report the synthetic method of magnetic nanoparticles which have excellent dispersity in the ETPTA resin mixture and the problem-solving process of mass fabrication method for fabricating micro-beads. Finally, I show improved assay results by reducing variations during lithography step and surface treatment step.

Chapter 2

Massive Synthesis Magnetic Nano-particles for Incorporating into Beads

To incorporate magnetic nanoparticles into micro-beads, there are several requirements: magnetic nanoparticles should be easily mixed in the ETPTA resin mixture and do not aggregate during lithography step. Moreover, it is desired to synthesize magnetic nanoparticles with high magnetic strength and high amount without complex purification procedure such as ultracentrifugation, size-exclusion chromatography, magnetic filtration, or flow field gradient. The superparamagentic materials satisfy almost these requirements, except mass productibility. These superparamagnetic nanoparticles exhibit magnetic characteristics only if external magnetic fields are exerted on them. Once the fields disappear, these marvelous materials loose magnetism.

Various chemical methods have been developed to synthesize magnetic nanoparticles including coprecipitation, microemulsions, hydrothermal reactions, hydrolysis and thermolysis of precursors, and sol-gel syntheses [6]. Most general method used for synthesis superparamagnetic nanoparticles is coprecipitation [7]. With this method, however, the control of particle size and size distribution is limited because only kinetic factors are controlling the growth of the crystal [6]. Also, reaction temperature of this synthesis method is too low to acquire high degree of crystallization and it result in low magnetic properties. Nanoparticles with a high level of mono-dispersity, size controllability, magnetism could be obtained by high-temperature decomposition of iron organic precursors. With this method, nanoparticles are dispersible in different organic solvents but probably not in water, and sophisticated post-preparative methods are required to make these nanoparticles water-soluble.

Instead of agglomeration of individual nanoparticles, depending on the progress of the reaction by being united themselves to form a colloidal nanocluster methods have been developed [8, 9]. Although theoretical principles of this method are well-established and the characteristics of these magnetic nanoclusters provide excellent magnetism and dispersity, it has limitation to mass production because these reactions are usually performed in reactors or autoclaves where the pressure is higher than 2000 psi and the temperature is above 200℃. Recently, there is a report

which incorporates a reflux system instead of autoclave system to perform solvothermal method [10]. With a reflux system, it was convenient to monitor changes in the reaction, isolate intermediates, and carry out large-scale synthesis of up to a few gram-scales. Because solvothermal system uses ethylene glycol as precursor solutions, it is possible to heat the reaction system up to 200℃ without autoclave or complicated apparatus and thus it is possible to acquire high degree of crystallization. However, magnetic nanoparticles which synthesized using this method show ferromagnetic characteristics and dispersity in the ETPTA resin mixture is too bad.

In this work, I introduce a solvothermal synthesis method using a reflux system which can synthesize superparamagnetic nanoparticles as well as ferromagnetic nanoparticles. Also, by introducing silica coating step, surface characteristics of magnetic nanoparticles could be controlled and dispersity in the resin mixture was improved.

2.1 Principles of Solvothermal Reduction Method

Solvothermal synthesis is very similar to the hydrothermal route, the only difference being that the precursor solution is usually not aqueous. In the

hydrothermal process, there are two main routes for the formation of ferrites: hydrolysis and oxidation. In the solvothermal reduction process, reduction process by reducing agent such as ethylene glycol occurs subsequently.

Magnetic precursor ($FeCl_3$, MCl_2 ; M= Co, Mn, Zn), sodium acetate, and distilled water are dissolved in the ethylene glycol which is one of a strong reducing agent with relatively high boiling point. Magnetic precursor is transformed to an amorphous gel via hydrolysis and condensation process. During this step, metal cations first transform from MClx to $M(OH)_2$ and $Fe(OH)_3$. As the reaction temperature is increased to boiling point of ethylene glycol, partial reduction of Fe^{3+} to Fe^{2+} occur via a reaction with ethylene glycol and an amorphous gel is transformed to a crystalline metal oxide, MFe_2O_4, which called magnetic nanoparticles through dehydration process [11]. The particle size in crystallization is controlled mainly through adjusting the processes rate of nucleation and grain growth. Nucleation might be faster than grain growth at higher temperatures and results in a decrease in grain size. Crystalline metal oxides are reduced by ethylene glycol what is one of strong reducing agents and agglomerated to a nanocluster

without any organic surface stabilizers or macromolecules as a crosslinking agent. These nanoclusters show excellent colloid stability in both aqueous and non-aqueous solution and it can be avoid to sophisticated surface treatment and resulting loss. In a typical solvothermal process, the diameters of the nanoclusters are influenced by the concentration of starting materials, solvent, temperature, and reaction time. The cluster size of MFe_2O_4 is proportional to precursor concentration, higher water content, reaction temperature, and reaction time whereas inversely proportional to organic ligand concentration. This simple approach provides a one-step, simple, general, and inexpensive method [8].

2.2 Experimental

$FeCl_3 \cdot 6H_2O$ (2.70 g, 10 mmol) was dissolved in 100 mL of ethylene glycol in a flask, followed by addition of sodium acetate (5.00 g), and distilled water (3 mL). The mixture was vigorously stirred at 70℃ for 30 min and then refluxed at 200℃ for 4~8 hours under a continuous flow of nitrogen gas. After cooling to room

temperature, the dark brown product was centrifuged at 1000 rpm for 30 min and washed several times with ethanol and distilled water to eliminate organic and inorganic byproducts. Finally, 740 mg (96% yield) of magnetic nanoparticles was obtained after drying at 60℃ for 6 h. This process can be extended to the synthesis of MFe_2O_4 (M=Co, Mn, Zn) by coprecipitation of M(II) and Fe(III) chlorides (M^{2+}/Fe^{3+}=0.5).

If silica coating was required, synthesized magnetic nanoparticles were dipped into DI water (3 mL), ethanol (20 mL) and ammonium hydroxide (28 %, 1 mL). Tetraethyl orthosilicate (TEOS) was injected into the solution with 0.3 mL/hr for 1 hour. The silica-coated magnetic nanoparticles were washed with ethanol 5 times.

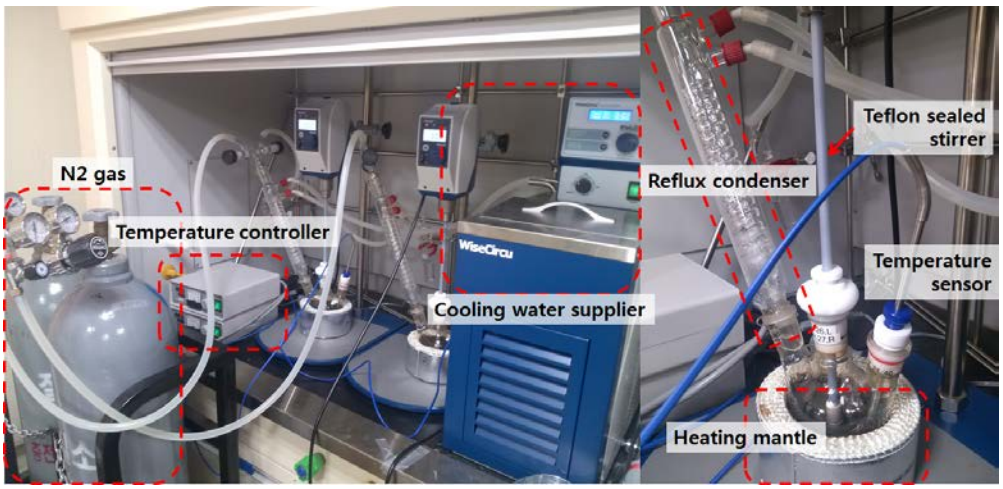

Figure 2.1 A picture of experimental setup.

2.3 Characteristics of Magnetic Nanoparticles which Synthesized in the Reflux System

Figure 2.2 shows the characteristics of the magnetic nanoparticles which have been synthesized with the reflux system. Figure 2.2 (A) and (B) show FE-SEM images at 20k and 200k magnification, respectively. These magnetic nanoparticles had cluster structure and its subunit size was smaller than 10 nm. Magnetism and surface charge of magnetic nanoparticles are shown in figure 2.2 (C) and (D). These

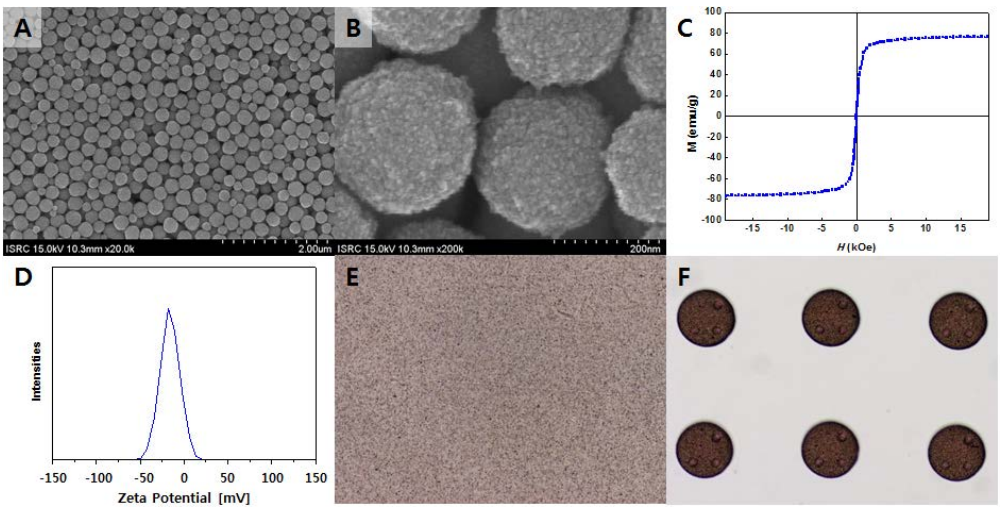

Figure 2.2 (A) A series of FE-SEM images of magnetic nanoparticles with magnification of 20k and (B) 200k. Nanoparticles are composed of small subunits. (C) Magnetization and (D) zeta-potential characteristics of magnetic nanoparticles. (E) Dispersity test image of magnetic nanoparticles in the resin mixture. (F) Image of the beads containing magnetic nanoparticles.

two characteristics are closely connected with dispersity in the resin mixture. To achieve excellent dispersity, attractive force has to be weak and repulsive force has to be strong. If magnetic nanoparticles have large hysteresis, it means strong attractive force even absence of external magnetic field and thus magnetic nanoparticles are severely aggregated. Unless magnetic nanoparticles are well dispersed in the resin mixture, multiplexed bioassays would be failed due to the variations which caused either in lithography step by scattering UV light or in decoding step by shading codes on the beads. Negative charge on the surface of nanoparticles act as repulsive force and the amount of charge could be manipulated via surface modification process such as silica coating. These magnetic nanoparticles show relatively high magnetization. Its saturation of magnetization value was about 77 emu/g while the saturation of magnetization of bulk Fe_3O_4 is 92 emu/g [12]. Also, this result is comparable with other solvothermal synthesis method using autoclave system [8, 9, 13]. Figure 2.2 (E) shows dispersity test result in the resin mixture. Fabricated beads using the resin mixture which contains magnetic nanoparticles are shown in figure 2.2 (F).

Figure 2.3 is a series of FE-SEM images of magnetic nanoparticles which prepared with different reaction times. In the reflux condition, a sufficient amount of Fe^{2+} was generated via the reduction of Fe^{3+} and ethylene glycol. When the

concentration of Fe^{2+} was higher than the threshold value, magnetite was generated at several sites within the amorpous gel, as indicated white spots in figure 2.3 (A) [10, 14]. As growing the nanoclusters, the remaining amorphous gel was consumed and finally only nanoclusters remained (figure 2.3 (B-D)). After 5 hours, there was no significant change in the sizes of magnetic nanoclusters.

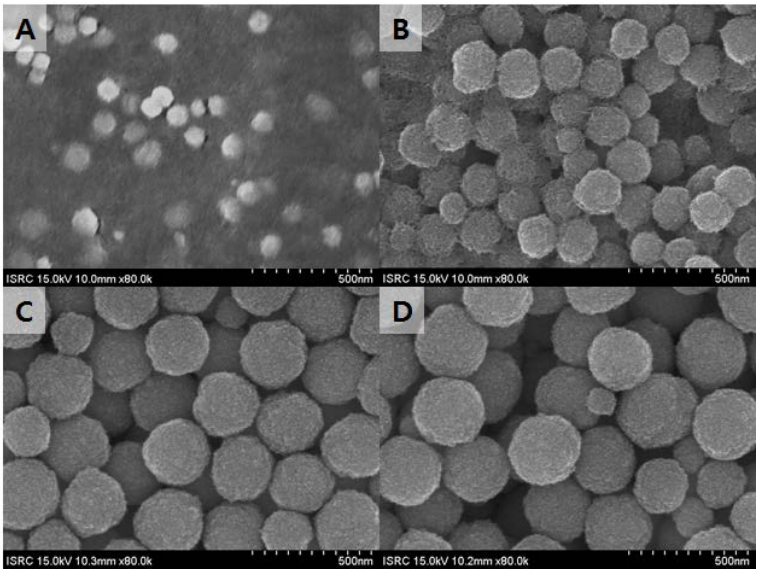

Figure 2.3 A series of FE-SEM images of magnetic nanoparticles prepared with different reaction times: (A) 2 h, (B) 3 h, (C) 5 h, and (D) 7 h.

In figure 2.3 (C) and (D), average diameter of nanoclusters was 240 nm and conventional magnetic ferrite particles which similar with this diameter show ferromagnetic characteristics. Other reported methods which incorporate reflux system and synthesize cluster structures also show ferromagnetic characteristics. In

general, an interaction between solvent and surface functional groups of magnetic nanoparticles, such as hydroxyl, is sufficient to overcome an attractive force of weak ferromagnetic characteristics. However, in our purpose, these magnetic nanoparticles must be perfectly dispersed because if magnetic nanoparticles are heterogeneously dispersed in the resin mixture then UV illumination energy to reach resin become uneven and thus it causes variation in assay process. Also, aggregated magnetic nanoparticles could cause error in code reading process.

In our system, however, it is possible to control not only diameter of cluster but also size of grain composing a nanocluster by simply adjusting the strength of a nitrogen flow during the formation of precursors. And, therefore, superparamagnteic and ferromagnetic nanoparticles can be selectively obtained through this size controllable process. Figure 2.4 shows the influence of nitrogen supply. Under a nitrogen supplying environment, water molecules in the reaction system would be removed. Since the ratio of water to metal ions cause different surface hydroxyl densities on the nanoparticle surface, the hydrolysis rate of $FeCl_3$ to Fe(OH)x could be controlled in the presence of specific amounts of water [13, 15]. It means that the size of subunit composing nanocluster could be controlled in the presence of specific amounts of water. In the presence of sufficient amounts of water, hydroxyl density on the surface would be increased and it leads to accelerate the growth speed of magnetic nanoparticles, and vice versa.

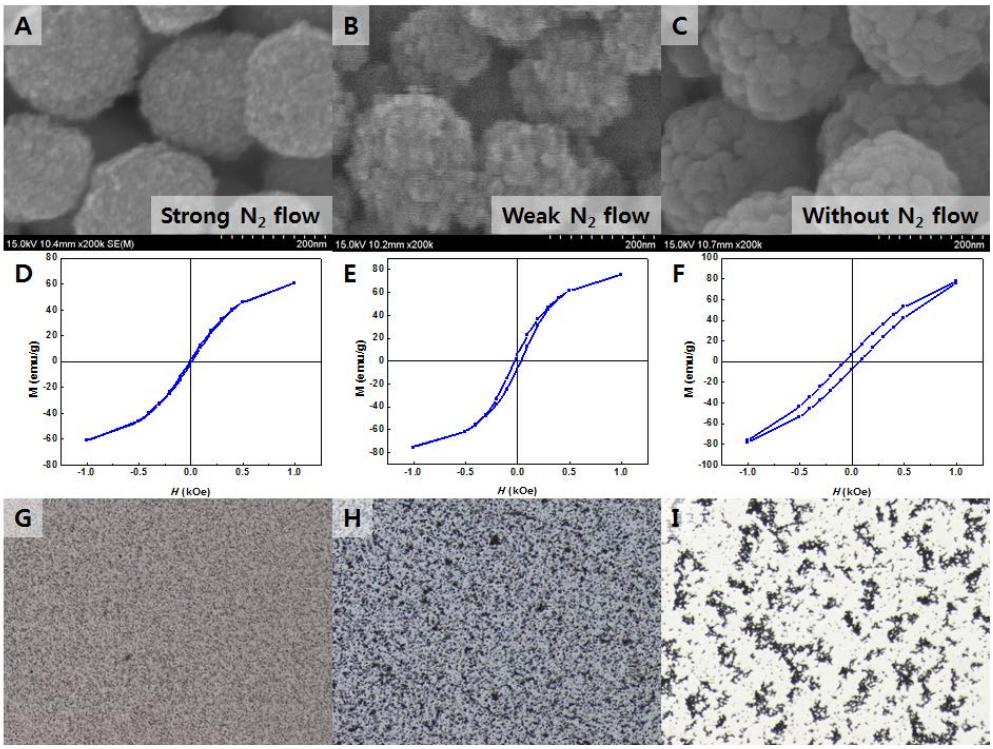

Figure 2.4 (A-C) FE-SEM images of magnetic nanoparticles synthesized under a different strength of nitrogen flow: (A) strong nitrogen flow, (B) weak nitrogen flow, and (C) without nitrogen flow. (D-F) VSM measurement results of magnetic nanoparticles shown in (A-C), respectively. (G-I) Dispersity test results of magnetic nanoparticles shown in (A-C), respectively.

With strong N_2 flow, the subunit size of nanocluster was smaller than 10 nm (figure 2.4A) whereas the subunits of without N_2 flow were larger than 30 nm (figure 2.4C). The critical size of criterion whether magnetic nanoparticles become superparamagnetic or not is known as 10 nm and, therefore, only magnetic

nanoparticles which synthesized under strong nitrogen flow show superparamagnetic characteristics. Vibrating sample magnetometer (VSM) graph shows the different hysteresis of them: figure 2.4 (D) corresponds to magnetic nanoparticles shown in figure 2.4 (A) while figure 2.4 (F) corresponds to figure 2.4 (C). Dispersity test results are shown in figure 2.4 (G-I). Understandably, nanoparticles synthesized under a strong nitrogen flow show better dispersity in resin mixture whereas nanoparticles synthesized without nitrogen gas supply show worst dispersity. To introduce magnetism to our beads, therefore, nitrogen gas supplying is essential in synthesis process. Also, supplying nitrogen gas protects against critical oxidation of the magnetite as well as control the subunit size [6].

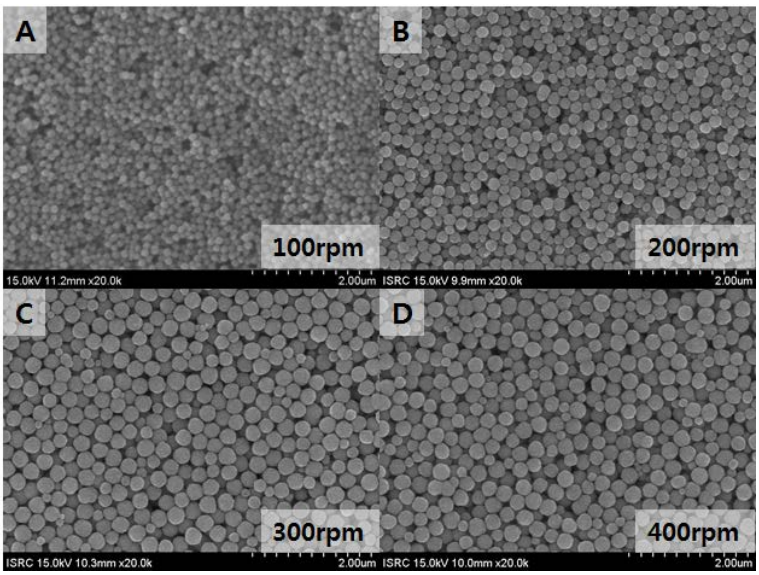

Figure 2.5 FE-SEM images of magnetic nanoparticles synthesized under a different stirring speed: (A) 100 rpm, (B) 200 rpm, (C) 300 rpm, and (D) 400 rpm.

In the conventional solvothermal synthesis, the diameter of nanoclusters is controlled by concentrations of precursor, concentration of surfactant, solvent type, reaction temperature and reaction time. In our reaction system, it is possible to control the sizes of nanoclusters and subunits by controlling stirring speed as well as above parameters. Figure 2.5 shows FE-SEM images of magnetic nanoparticles synthesized under a different stirring speed. Effects of rapid stirring are not only making homogeneous temperature and concentration of materials in the reaction chamber. More vigorous stirring provides more chance to meet among the Fe_3O_4 nucleates. As increase stirring speed, a diameter of magnetic nanoclusters was increased, and vice versa. There was saturation stirring speed that nanoclusters did not grow anymore because almost all nucleates were already agglomerated to nanoclusters in same reaction time.

Dispersity of magnetic nanoparticles in the ETPTA resin mixture could be improved by incorporating silica coating process [9, 16]. Magnetic nanoparticles shown in figure 2.6 (B) were silica coated and showed better dispersity in the resin mixture (figure 2.6 (D)). Figure 2.6 (C-D) shows the shifted zeta-potential value by silica coating. Zeta-potential indicates the degree of repulsive force between nanoparticles and thus it is closely related to the stability of colloidal dispersions.

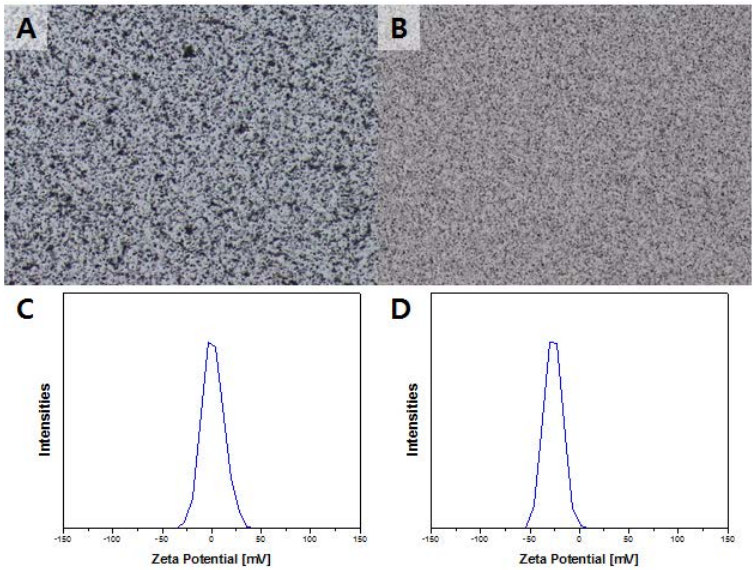

Figure 2.6 (A) Dispersity test image of magnetic nanoparticles synthesized under a weak nitrogen flow. (B) Dispersity test image of silica coated magnetic nanoparticles used in (A). (C) zeta-potential of bare magnetic nanoparticles and (D) silica coated magnetic nanoparticles.

Colloids with high zeta potential (negative or positive) are electrically stabilized while colloids with low zeta potentials tend to aggregated [17]. Because silica has more electron affinity than iron molecules, silica attracts more electrons in a solvent and thus Si-OH terminated surface has more negative charges than Fe-OH terminated surface. More negatively charged surface act as repulsive force between magnetic nanoparticles and thus it shows better dispersity in resin mixture.

Figure 2.7 shows a series of FE-SEM images of silica-coated magnetic nanoparticles according to the amount of TEOS injected. Magnetic nanoparticles shown in figure 2.4 (A) were silica coated with different amount of TEOS. With

more amounts of TEOS, thickness of silica shell formed on the magnetic nanoparticles surface was increased and grains composing cluster were eventually covered. More silica on the magnetic nanoparticles attracts more negative charges and thus dispersity was improved with stronger repulsive force. However, too much amount of TEOS generates silica nanoparticles or glues the nanoclusters and thus dispersity was degenerated.

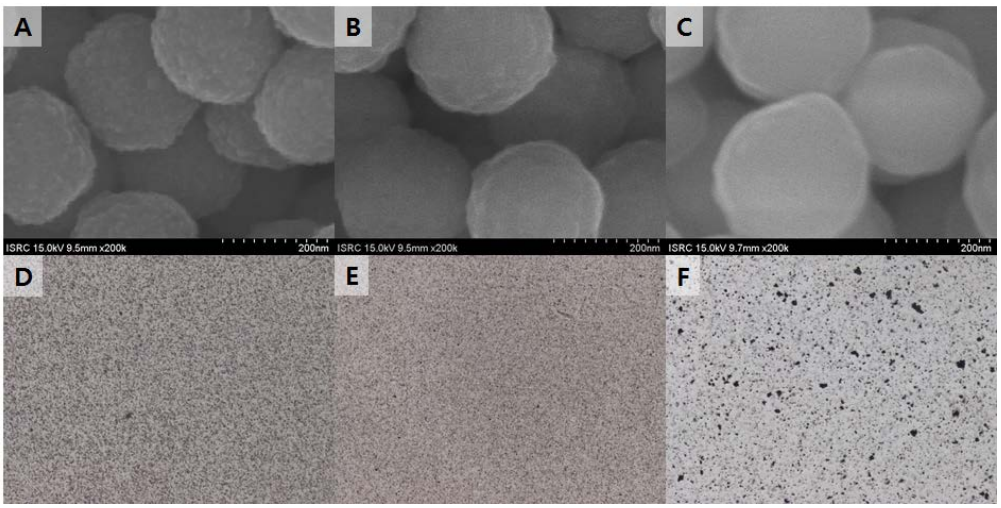

Figure 2.7 (A-C) A series of FE-SEM images of silica coated magnetic nanoparticles prepared under a different amounts of TEOS injection: (A) 100 μL, (B) 200 μL, and (C) 400 μL. (D-F) Dispersity test results of magnetic nanoparticles shown in (A-C).

In summary, magnetic nanoparticles were easily synthesized via the simple reaction of $FeCl_3 \cdot 6H_2O$, sodium acetate, diltilled water, and ethylene glycol in the

reflux system. Ferromagnetic and superparamagnetic magnetic nanoparticles were selectively obtained by simple adjusting the strength of nitrogen flow. Because one of main purpose of our magnetic nanoparticles is incorporating to micro-beads for multiplexed bioassays, magnetic nanoparticles have to possess excellent dispersity in the ETPTA resin mixture. Sometimes, only superparamagnetic characteristic which means weak attractive force does not sufficient to satisfy this criterion. By introducing silica coating process, it is possible to provide strong repulsive force and thus excellent dispersity could be achieved. Also, these magnetic nanoparticles could be used not only as magnetic separator of the beads in a suspension but also as nano-beads for bioassays such as targeted druge delivery, bio-molecular separations, magnetic resonance image, and so on.

Chapter 3

Development of Mass Fabrication Method for Encoded Magnetic Beads

In this chapter, I introduce an overall process of mass fabrication of encoded micro-beads and an influence of parameters at each procedure. This fabrication method can be considered as conventional semiconductor fabrication process, but there are a few additional parameters have to be considered because the UV curable resin mixture has different characteristics with conventional PR. Solvent of this resin mixture is not removable by thermal or vacuum process and this characteristic disables the height control method using spin coating process. Also, the resins are not solidified before UV lithography step and this liquid resin fills a micro-sized gap, capillary flow causes various problematic phenomena. Sometimes, unexposed region of the resin mixture is cured because energy penetration through resin. This characteristics

also affect to the size of the beads according to distance from glass edge or between neighboring beads even if same exposure energy is illuminated.

In this chapter, I introduce the procedure of control and optimize of parameters to solve these problems. With this mass fabrication method, it is possible to increase the number of beads which can be fabricated in 6 hours from 110,000 to 3,360,000 in case of 100 μm sized beads.

3.1 Overall Procedure of Bead Fabrication

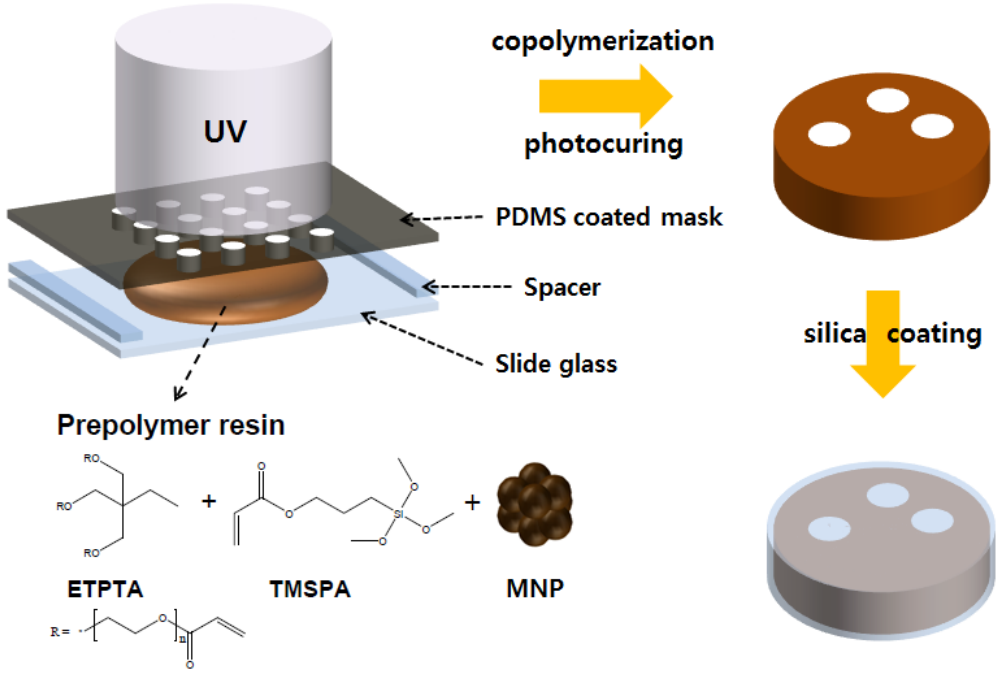

Figure 3.1 A conceptual description of encoded magnetic beads fabrication process for multiplexed bioassays.

Figure 3.1 shows overall procedure of producing silica-coated encoded magnetic micro-beads. In order to fabricate encoded polymeric beads, the resin mixture consisted of 10 : 1 : 1 volume ratio of trimethylolpropane ethoxylate triacrylate (ETPTA) and 3-(trimethoxysilyl)propyl acrylate (TMSPA) and 2-hydroxy-2-methylpropiophenone (DAROCUR) was prepared as a UV curable material. ETPTA is a main structure of encoded micro-beads by composing acrylate matrix. TMSPA serves silicon-centered group which can be formed as silica seed. If it is required, magnetic nanoparticles were added to this mixture. This resin mixture was vigorously vortexed for 1 hour and loaded on the polydimethylsiloxane (PDMS) coated photo-mask. PDMS coated surface provides the oxygen inhibition layer which prevents the photo-polymerization process and thus polymerized beads are not stick to this photo mask [2, 18]. Spacers were placed on the both ends of the photo mask and a height of disk-shaped micro-beads was controlled by adjusting the thickness of spacer. Then, the slide glass either PDMS coated or not was covered on them. The space between the two glass slides was filled with the resin mixture of ETPTA, TMSPA, DAROCUR and magnetic nanoparticles. The assembled parts were placed on the UV exposure machine. The encoded polymeric beads were fabricated by UV illuminating to these assemblies. Then, photo-mask and slide glass were separated. If bare slide glass was used in previous step, beads were attached to

slide glass. After washing with ethanol to remove uncured resin, beads were detached using knife and collected in a tube. If PDMS coated glass was used in previous step, beads were collect in a tube while separate photo-mask and slide glass because beads were not attached to slide glass. To remove uncured resin perfectly, we performed three times washing with ethanol and then carried out silica coating on the beads through a modified Stöber method [16, 19]. This method enables millions of beads to be coated in a single step. The thickness of the silica layer could be controlled in a straightforward fashion via controlling concentrations of precursors and reaction time.

3.2 Factors that Affect to Bead Fabrication Process

There are several problems with conventional contact mask lithography method to fabricate our beads because the resin mixture used in this work has different characteristics from the conventional PR. As mentioned above, height control mechanism using spin coating process is not adaptable with our resin mixture because the solvent of resin is not removable by thermal or vacuum method. Also, because of the resin mixture is not solidified and a space between photo mask and slide glass is micrometer dimension, capillary flow would be generated. Figure

3.2 shows the problematic phenomena when capillary flow is not removed.

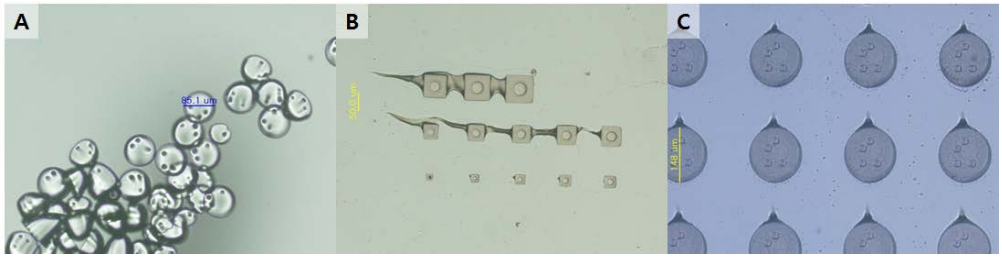

Figure 3.2 Problematic phenomena caused by capillary flow of resin: (A) deformed beads, (B) bridges, and (C) tails.

If both photo mask and slide glass were both PDMS coated, polymerized resin was carried away by the capillary flow during UV exposure process and shapes of beads were deformed (figure 3.2 (A)). This problem is resoluble by removing capillary force or using bare slide glass. On the bare slide glasses which were not coated with PDMS, photo-polymerization process could be occurred and thus cured beads were attached on the slide glass. Figure 3.2 (B) and (C) show the results of using bare slide glass but capillary flow was still existent. These results signify needs for completely remove the capillary flow.

To remove capillary flow, we were removed empty space where capillary flow arrives. An excess amount of resin was loaded on the photo mask and covered slide glass was pushed strongly. During this step, the resin mixture filled a space between photo mask and slide glass and spare amount of resin was flooded and

made drops at the edge of space. If these drops are not removed, capillary force drives resin flow from inside to outside of the space and total amount of resin in the space would be insufficient. By removing these drops rapidly, capillary barrier was made at the edge of space and capillary flow was stopped. There is another mechanism of resin flow. During polymerization process, the resin mixture is slightly shrunk and it also generate partial flow [20]. However, this phenomenon is occurred at all over the UV exposed region and thus net flow become zero.

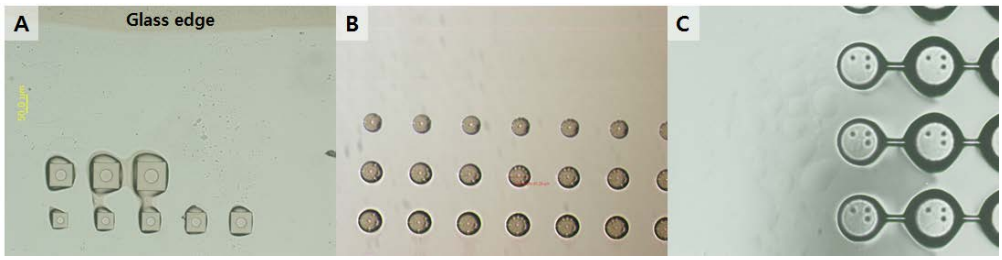

Figure 3.3 Problematic phenomena caused by energy penetration through the resin: (A) Exposure area was close to glass edge. (B) Exposure area was far from glass edge and distance between the beads was far from each other. (C) Exposure area was far from glass edge and distance between the beads was too short.

Another problematic characteristic of the ETPTA resin mixture is energy penetration through resin. If UV exposure region was close to glass edge, penetrated energy from glass edge affected to photo-polymerization process and most outer region was over-cured (figure 3.3 (A)). On the other hand, if UV exposure region was far from glass edge, penetrated energy from glass edge was negligible. However,

in contrast to the previous case, most outer region was under-cured nevertheless same amount of UV energy was illuminated because UV illumination energy was penetrated not only from glass edge but also from neighboring beads (figure 3.3 (B)). The beads located at inner region received the penetrated energy from every side of neighboring beads while the beads located at most outer region received half amount of penetrated energy. Also, unintended interference was occurred if the distance between beads was too close (figure 3.3 (C)).

There are several methods to solve this problem: increasing distance between the beads to reduce the effect of penetrated energy, increasing the size of most outer beads to compensate the lack of penetrated energy, optimizing distance between most outer beads and glass edge to find equilibrium point, and placing additional structure besides to most outer beads to provide same amount of UV illumination energy. A method what we adopted is placing additional beads. These beads do not have any codes so they are not read by decoding software. Also, the population of these beads is only ~1 %.

Figure 3.4 shows test results of distance between beads to beads. Purpose of this test is to find trade-off distance which increases a yield of number of the beads at certain area while unintended interferences such as bridge formation are not occurred. In case of 100 μm beads, the minimum distance which not made bridge between beads was about 85 μm. Existence of magnetic nanoparticles did not

exercised great influence on this value. Also, we can observed that diameter of beads were decreased as distance between the beads was increased. This tendency was another evidence of energy penetration between neighboring beads.

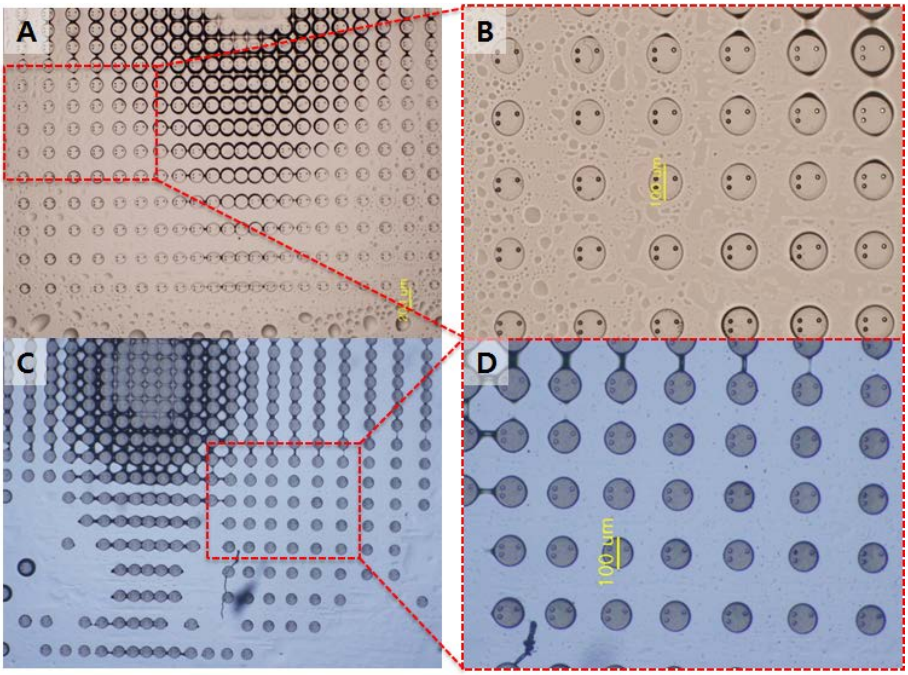

Figure 3.4 Test results of distance between beads for (A) non-magnetic and (B) magnetic beads.

Figure 3.5 shows resolution test results. In figure 3.5 (A) and (B), embossed pattern was observed up to 5 μm while engraved pattern was observed up to 3 μm with a microscope of 100 magnification (smaller pattern was not observed in both case). Fortunately, existence of magnetic nanoparticles did not affect to

resolution test results. Figure 3.5 (C) and (D) show the results of dot code resolution and line code resolution with 100 μm sized beads, respectively. Resolution limits were 4 μm for dot code and 3 μm for line code with a microscope of 100 magnification and code analysis software which developed ourselves.

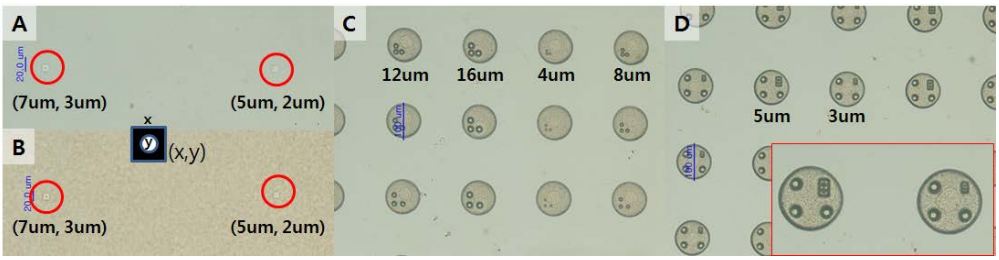

Figure 3.5 Resolution test results of the resin mixture.

3.3 Optimizing the Concentration of Magnetic Nanoparticles in the Resin Mixture

Incorporating magnetic materials into the beads provide useful tool to enable an active magnetic separation of the beads from a suspension solution. By applying an external magnetic field to a solution, a mixture containing magnetic beads as well as the biomolecules bound to those beads could be selectively sorted from the solution mixture. The magnetic manipulation of the free-floating magnetic beads could be useful for bioassays involving a solution exchange.

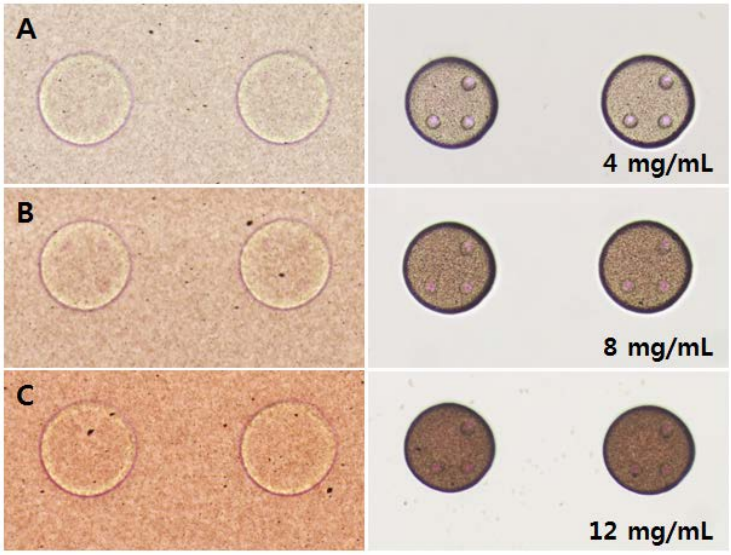

Figure 3.6 Lithography test results for the resin mixture with different concentration of magnetic nanoparticles: (A) 4 mg/mL, (B) 8 mg/mL, and (C) 12 mg/mL.

Figure 3.6 shows the lithography results for each resin mixture containing different concentration of magnetic nanoparticles: 4 mg/mL, 8 mg/mL, and 12 mg/, respectively. UV exposure energy was increased as increased concentration of magnetic nanoparticles. In 12 mg/mL case, codes on the beads were hard to recognize using image analysis program and thus it was recommended that the concentration of magnetic nanoparticles should be lower than 12 mg/mL.

Gravity force which affect to the 100 μm sized beads is about $2.56 * 10^{-9}\,N$. It means that magnetic force between the beads and external magnetic fields has to be larger than $2.56 * 10^{-9}\,N$. Magnetic fields strength of

conventional magnet is sufficient to hold the beads even if the concentration of magnetic nanoparticles is lower than 2 mg/mL. However, magnetic fields strength of 96-well patterned magnet plate is much weaker than conventional magnet. In other words, if it is possible to hold the beads with 96-well patterned magnet plate then magnetic beads are always to be held by magnet.

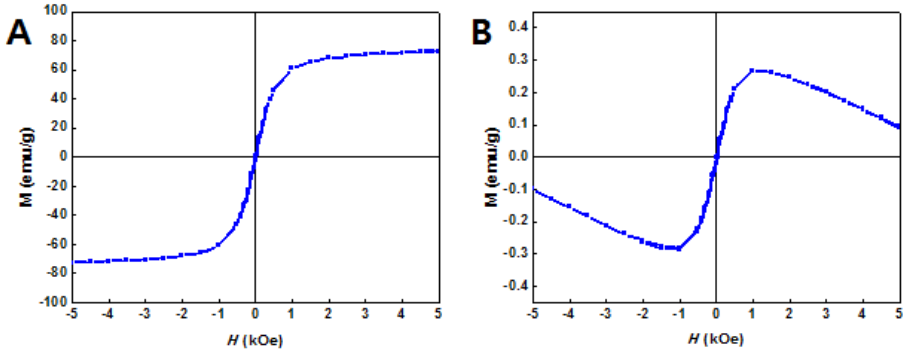

Figure 3.7 Magnetization curves (M-H curves) obtained by VSM (a) magnetic nanoparticles (b) magnetic containing micro-beads.

Magnetic micro-beads consist of magnetic nanoparticles surrounded by an ETPTA polymer matrix. Because ETPTA is one of diamagnetic materials, magnetic properties of magnetic micro-beads are affected both magnetic nanoparticles and ETPTA polymer matrix. First, magnetization curve of magnetic nanoparticles, shown in figure 3.7 (A), can be approximated as a Langevin function [21].

$$\mathrm{m} = M_s\left\{coth\left(\frac{g\mu_B B}{k_B T}\right) - \frac{k_B T}{g\mu_B B}\right\}$$

where Ms stands for saturation magnetization, g for g-factor, μ_B for Bohr magneton, B for applied magnetic field, k_B for Boltzman constant, and T for temperature. Second, the diamagnetic susceptibility of an ETPTA polymer matrix was calculated from the measured data shown in figure 3.7 (B), and the result is $-5.31 \cdot 10^{-5}$ emu/Oe·g. These two magnetic characteristics are responsible for the overall magnetic characteristics of the beads. A modified Langevin function is obtained from linear superposition of previously achieved functions,

$$\mathrm{m}' = w \cdot M_s \left\{ coth\left(\frac{g\mu_B B}{k_B T}\right) - \frac{k_B T}{g\mu_B B} \right\} + (1-w) \cdot \chi_{dia} \cdot B$$

where w stands for weight percentage of magnetic nanoparticles and χ_{dia} for the diamagnetic susceptibility of the ETPTA polymer matrix. Finally, magnetic force between the beads and magnet plate is calculated through magnetic force equation, $\mathrm{F} = \nabla(\mathrm{m} \cdot \mathrm{B})$.

The maximum solution volume in assay protocol was 100 μL, and height of a solution in the 96-well plate is about 2.6 mm. Magnetic fields strength which affect to 2.6 mm apart from magnet plate was 0.46 kG. In this condition, to acquire magnetic force larger than gravity force, $2.56 \cdot 10^{-9}\ N$, the beads should have more than 2.48 wt% of magnetic nanoparticles and this value corresponds to the concentration of 27.24 mg/mL. In this concentration, as mentioned above, codes on the beads will be not distinguishable. Fortunately, the beads sink to the bottom of the well plate because polymeric beads have more weight and higher density compare

with water or other solution molecules. If the beads contain magnetic nanoparticles, then sinking speed become faster. If the beads sink till 1 mm from magnet plate, magnetic force between the beads and magnet plate is larger than gravity force even with the beads containing 0.29 wt% of magnetic nanoparticles. This value corresponds to concentration of 3.21 mg/mL.

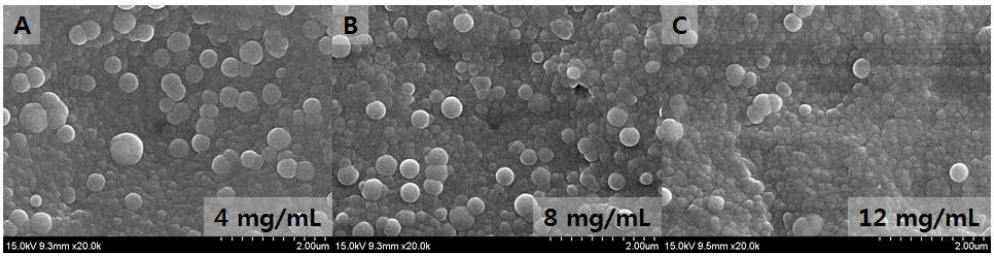

Figure 3.8 A series of FE-SEM images of silica-coated beads prepared with different concentration of magnetic nanoparticles: (A) 4 mg/mL, (B) 8 mg/mL, and (C) 12 mg/mL.

Figure 3.8 shows a series of FE-SEM images of silica-coated micro beads according to magnetic nanoparticles content. The beads were fabricated with the resin mixtures containing 4mg/mL, 8mg/mL, and 12mg/mL of magnetic nanoparticles and other conditions were same. There were no noticeable differences as increased of magnetic nanoparticles content. It means that the amount of magnetic nanoparticles in the beads will not affect to assay results by its own property except magnetism.

In summary, the concentration of magnetic nanoparticles should be higher than 3.21 mg/mL for effective magnetic separation with 96-well patterned magnet plate and should be lower than 12 mg/mL for code recognition.

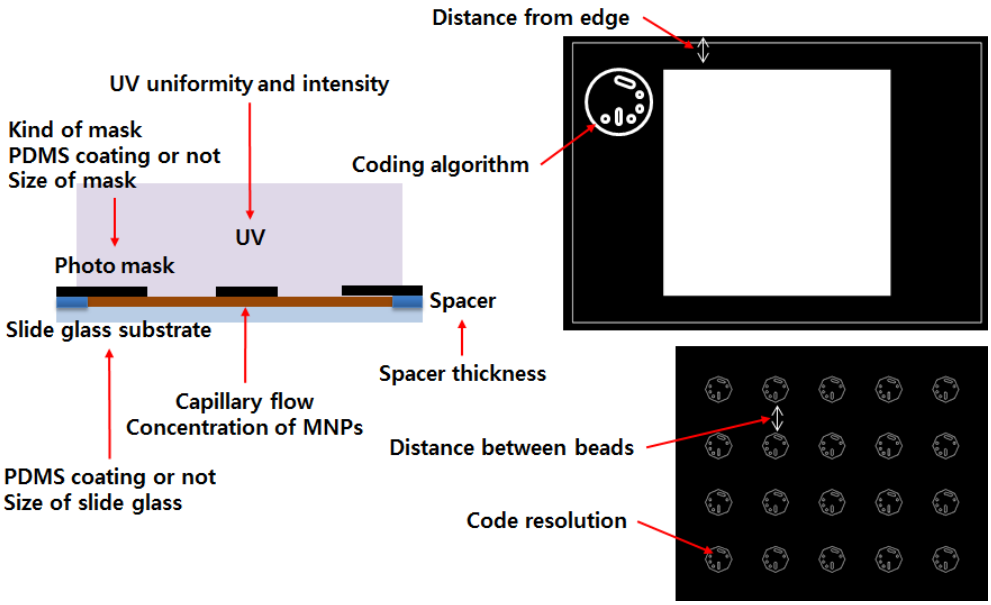

Figure 3.9 Summarized diagram of parameters which affect to bead fabrication.

Parameters which have to be considered are surmised in figure 3.9. We optimized that surface modification protocol of photo mask and slide glass, amount of resin which loading in the space between photo mask and slide glass, capillary flow restriction, distance from glass edge to UV exposure region, distance between beads, code resolution and algorithm, concentration of magnetic nanoparticles, and so on.

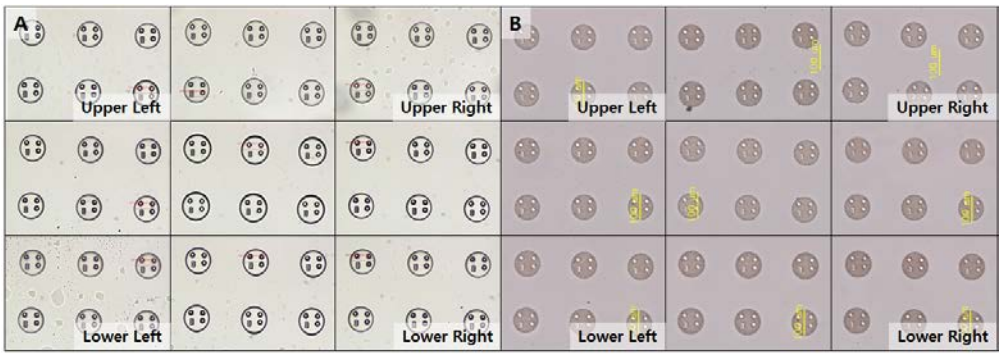

Figure 3.10 Images of mass fabricated beads for (A) non-magnetic and (B) magnetic.

Considering the above all parameters, we can obtained the results shown in figure 3.10. With this method, we drastically increased the number of beads about 30 times compare with previous method. We can fabricate 140,000 beads which have 100 μm diameter at one cycle, and three million beads can be fabricated in 6 hours. Fabricated beads were coated with silica through a modified Stöber method [16, 19].

Chapter 4

Assay Results using Mass Fabricated Encoded Magnetic Beads

The silica-coated encoded magnetic beads were fabricated as described in Chapter 3. Our silica-coated encoded magnetic micro-beads provide useful benefits for multiplexed bioassays. The graphical codes of beads indicate the identity of probe types on the surface of beads. Silica coating procedure not only gives chemical and mechanical stability but also enables to directly adopt well-established silica surface chemistry such as introduction of carboxyl or amine groups which can form covalent bond with various biomolecules [4, 5]. Hydroxyl groups of a silica surface were reacted with 3-aminopropyltriethoxysilane (APTES) and it derived primary amine groups. These amines were subsequently reacted to the succinic anhydride, resulting in carboxylated surfaces which able to immobilize amine modified DNA or antibody.

In previous works, there are some demonstrations of multiplexed DNA hybridization assay and multiplexed cytokine assay using our beads (will be published).

In this chapter, I will show the human papillomavirus (HPV) genotyping assay results using mass fabricated magnetic beads and compare with previous results which used OFML fabricated nonmagnetic beads. The accurate identification of high-risk HPV genotypes in mixed infections is important for defining woman's risk for progression to cervical cancer [22].

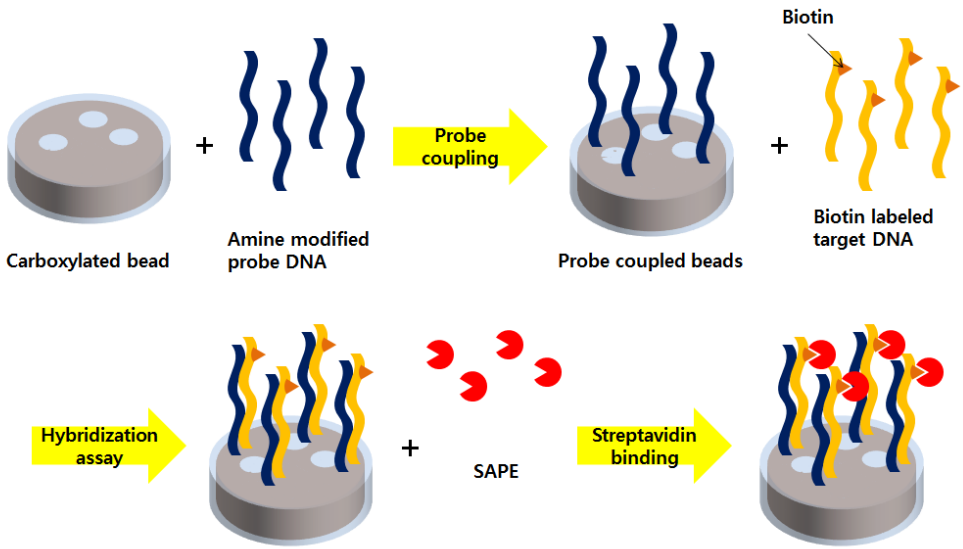

Figure 4.1 A conceptual scheme of DNA hybridization assay protocol.

A conceptual scheme of DNA hybridization assay is shown in Figure 4.1. The carboxylic group on the beads surface and the amino group of the amino-terminated probe DNA formed an amide bond by a cross-linking process. Then,

target HPV gene sequences were added and incubated. HPV target genes were prepared with the 2-step PCR process: first PCR step is for the amplification and second PCR step is for the labeling with biotin-attached dCTP. After the hybridization assay, fluorescent dye-labeled streptavidins were introduced to acquire fluorescent signals. Then, bright-field and fluorescence microscope images were obtained for the analysis.

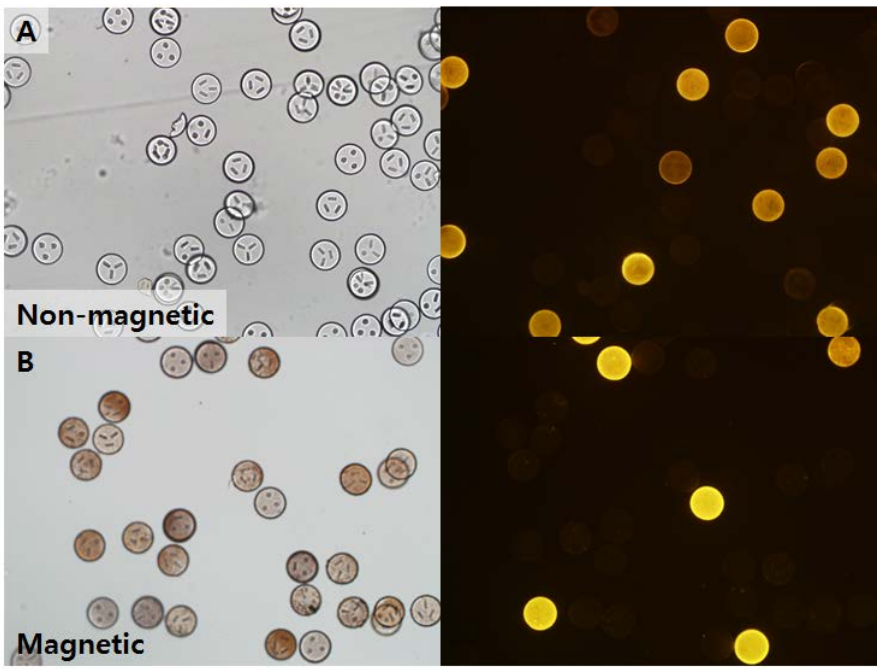

Figure 4.2 HPV genotyping assay results of (A) non-magnetic beads and (B) magnetic beads.

Figure 4.2 shows improved results by incorporating magnetic nanoparticles

and stabilizing bead fabrication process. As shown in fluorescent images (figure 4.2), only the beads with probes complementary to the specific target sequences exhibited obvious fluorescence in the presence of other probe-attached beads. Because DNA hybridization assay is one of on/off signal assay, the fluorescence intensity of all those beads has to be same. Signal intensities of non-magnetic beads differ from bead to bead (figure 4.2 (A)) whereas magnetic beads show more even fluorescence intensity (figure 4.2 (B)).

(A) Non-magnetic Bead

HPV type	HPV type-specific probe						
	6	**11**	**18**	**31**	**33**	**42**	**59**
6	**130.4**	10.1	9.8	8.7	12.9	8.9	8.4
11	7.9	**90.5**	8.0	7.4	8.0	7.5	10.0
18	10.4	12.6	**162.0**	8.7	12.0	15.8	12.9
31	5.9	4.0	7.1	**126.6**	3.5	5.9	5.4
33	3.4	5.1	3.7	4.2	**172.4**	3.5	3.4
42	9.6	9.7	8.6	9.7	9.0	**103.7**	10.6
59	4.3	3.1	3.0	3.1	2.3	3.6	**134.2**

(B) Magnetic Bead

HPV type	HPV type-specific probe						
	6	**11**	**18**	**31**	**33**	**42**	**59**
6	**186.8**	5.3	4.6	4.7	6.6	6.7	4.8
11	7.6	**161.4**	6.5	8.0	9.0	8.8	9.1
18	11.8	12.3	**179.2**	11.0	11.5	12.3	13.9
31	9.0	8.3	9.9	**170.5**	10.5	7.4	10.2
33	5.9	5.6	6.0	5.8	**142.0**	7.1	5.4
42	7.8	3.4	9.1	4.6	7.8	**165.2**	5.0
59	7.6	7.2	9.2	8.3	7.5	10.1	**184.2**

Table 1 Comparison of assay results of (A) non-magnetic and (B) magnetic beads.

Fluorescence intensities of the all beads were measured using our own software to verify sensitivity and cross hybridization. A conventionally used image processing method was customized to detect fluorescent signals in the images. Results of 7 types of HPV were shown in Table 1. The beads accurately identified each target HPV gene with negligible cross-hybridization noise and non-specific binding in both magnetic and non-magnetic beads. Signal intensities of magnetic beads were always higher than that of non-magnetic beads except HPV 33 case. These results show that introducing magnetic nanoparticles to the beads enhances the reactivity as well as provides more convenience.

Chapter 5

Conclusion

This thesis presented a developing pathway for mass fabrication of encoded magnetic micro-beads to achieve more reliable and reproducible bioassay results.

In chapter 2, a solvothermal reduction method which incorporates refluxing system instead of autoclave system was presented. To synthesize magnetic nanoparticles which have excellent dispersity in the ETPTA resin mixture, characteristics of superparamagnetic and high surface charge density were required. In this synthesis method, superparamagnetic and ferromagnetic nanoparticles were selectively synthesized by simple adjusting nitrogen flow strength. Also, by introducing silica coating step, negative charges on the surface of magnetic nanoparticles could be increased and thus repulsive force between magnetic nanoparticles was increased. This results in not only better dispersity of magnetic nanoparticles but also open the possibility to be utilized as nano-beads for bioassays.

As an application, and as a one of main purpose, magnetic nanoparticles were contained to micro-beads for active magnetic separation of the beads in a suspension solution.

A mass fabrication method for encoded micro-beads was presented in chapter 3. Because UV curable resin which used in this works has difference characteristics with conventional PR, much more parameters had to be considered to utilize large area UV lithography. Capillary flow restriction and energy penetration through resin were key factors. Incorporating magnetic nanoparticles required more UV illumination energy but it did not affect to resolution or optimum distance between beads. Also, this method does not require realignment at each operation as well as could produce much more beads in one cycle. These advantages resulted in not only reducing the working time to fabricate same number of beads but also reducing bead to bead variation. With this method, we drastically increased the number of beads about 30 times compare with previous method. We can fabricate 140,000 beads which have 100um diameter at one cycle, and three million beads can be fabricated in 6 hours.

In chapter 4, drastically improved HPV gene genotyping assay results by incorporating magnetic nanoparticles and stabilizing lithography process of micro-beads were shown. There were negligible cross-hybridization and non-specific adsorption of analyte with increased signal to noise ratio.

Bibliography

[1] S. Birtwell and H. Morgan, "Microparticle encoding technologies for high-throughput multiplexed suspension assays," *Integrative Biology,* vol. 1, pp. 345-362, Jun 2009. [국제저널지]

[2] S. E. Chung, *et al.*, "Optofluidic maskless lithography system for real-time synthesis of photopolymerized microstructures in microfluidic channels," *Applied Physics Letters,* vol. 91, Jul 23 2007. [국제저널지]

[3] S. Han, *et al.*, "Lithographically Encoded Polymer Microtaggant Using High-Capacity and Error-Correctable QR Code for Anti-Counterfeiting of Drugs," *Advanced Materials,* vol. 24, pp. 5924-+ , Nov 20 2012. [국제저널지]

[4] L. R. Hilliard, *et al.*, "Immobilization of oligonucleotides onto silica nanoparticles for DNA hybridization studies," *Analytica Chimica Acta,* vol. 470, pp. 51-56, Oct 11 2002. [국제저널지]

[5] Y. H. Rogers, *et al.*, "Immobilization of oligonucleotides onto a glass support via disulfide bonds: A method for preparation of

DNA microarrays," *Analytical Biochemistry,* vol. 266, pp. 23-30, Jan 1 1999. [국제저널지]

[6] S. Laurent, *et al.*, "Magnetic iron oxide nanoparticles: Synthesis, stabilization, vectorization, physicochemical characterizations, and biological applications," *Chemical Reviews,* vol. 108, pp. 2064-2110, Jun 2008. [국제저널지]

[7] A. F. C. Campos, *et al.*, "Nanoparticles superficial density of charge in electric double-layered magnetic fluid: A conductimetric and potentiometric approach," *European Physical Journal E,* vol. 6, pp. 29-35, Sep 2001. [국제저널지]

[8] H. Deng, *et al.*, "Monodisperse magnetic single-crystal ferrite microspheres," *Angewandte Chemie-International Edition,* vol. 44, pp. 2782-2785, 2005. [국제저널지]

[9] J. P. Ge, *et al.*, "Highly tunable superparamagnetic colloidal photonic crystals," *Angewandte Chemie-International Edition,* vol. 46, pp. 7428-7431, 2007. [국제저널지]

[10] J. Cha, *et al.*, "Solid-state phase transformation mechanism for formation of magnetic multi-granule nanoclusters," *Rsc Advances,* vol. 3, pp. 3631-3637, 2013. [국제저널지]

[11] S. W. Cao, *et al.*, "Fe3O4 polyhedral nanoparticles with a high magnetization synthesized in mixed solvent ethylene glycol-water system," *New Journal of Chemistry,* vol. 32, pp. 1526-1530, Sep 2008. [국제저널지]

[12] B. D. Cullity and C. D. Graham, *Introduction to magnetic materials*, 2nd ed. Hoboken, N.J.: IEEE/Wiley, 2009. [국제저널지]

[13] S. H. Xuan, *et al.*, "Facile synthesis of size-controllable monodispersed ferrite nanospheres," *Journal of Materials Chemistry,* vol. 20, pp. 5086-5094, 2010. [국제저널지]

[14] C. M. Hansel, *et al.*, "Secondary mineralization pathways induced by dissimilatory iron reduction of ferrihydrite under advective flow," *Geochimica Et Cosmochimica Acta,* vol. 67, pp. 2977-2992, Aug 2003. [국제저널지]

[15] T. He, *et al.*, "Controlled synthesis of Co3O4 nanoparticles through oriented aggregation," *Chemistry of Materials,* vol. 16, pp. 737-743, Feb 24 2004. [국제저널지]

[16] J. P. Ge and Y. D. Yin, "Magnetically tunable colloidal photonic structures in alkanol solutions," *Advanced Materials,* vol. 20, pp. 3485-+ , Sep 17 2008. [국제저널지]

[17] D. Hanaor, *et al.*, "The effects of carboxylic acids on the aqueous dispersion and electrophoretic deposition of ZrO2," *Journal of the European Ceramic Society,* vol. 32, pp. 235-244, Jan 2012. [국제저널지]

[18] D. Dendukuri, *et al.*, "Continuous-flow lithography for high-throughput microparticle synthesis," *Nature Materials,* vol. 5, pp. 365-369, May 2006. [국제저널지]

[19] W. Stober, *et al.*, "Controlled Growth of Monodisperse Silica Spheres in Micron Size Range," *Journal of Colloid and Interface Science,* vol. 26, pp. 62-&, 1968. [국제저널지]

[20] H. Kim, *et al.*, "Structural colour printing using a magnetically tunable and lithographically fixable photonic crystal," *Nature Photonics,* vol. 3, pp. 534-540, Sep 2009. [국제저널지]

[21] H. Lee, *et al.*, "Colour-barcoded magnetic microparticles for multiplexed bioassays," *Nature Materials,* vol. 9, pp. 745-749, Sep 2010. [국제저널지]

[22] Y. Oh, *et al.*, "Polymerase chain reaction-based fluorescent Luminex assay to detect the presence of human papillomavirus types," *Cancer Science,* vol. 98, pp. 549-554, Apr 2007. [국제저널지]

다중화 바이오 어세이를 위한 코드화된 자성 입자 양산 방법 개발

하나의 샘플을 여러 가지 프로브 분자와 동시에 반응시키는 다중화 어세이 기술을 통해 연구자들은 보다 많은 양의 정보를 얻을 수 있다. 다중화 어세이는 시약의 양, 실험 시간, 노동집약적인 작업 등을 크게 줄일 수 있어 유전형질을 분석하거나 약물의 효과를 검증할 때, 병을 진단할 때 등에 유용하게 사용되는 기술이다. 소속 연구실에서는 코드화된 마이크로 입자에 기반한 다중화 어세이 기술을 개발해 왔으며, 이를 이용한 DNA 유전자형 검사, 효소결합 면역흡착 분석, 단백질 검출 검사 등에 성공하였다. 하지만 좀더 신뢰 할만 하고 재현성 있는 결과를 얻기 위해 개선해야 하는 부분들이 남아있다. 통계적으로 유의한 수준의 충분한 데이터를 확보하기 위해서는 코드화된 마이크로 입자의 생산량을 늘릴 필요가 있으며, 입자의 생산 및 표면 처리 과정에서 발생하는 입자간 차이를 줄여야 한다.

이 논문에서는 위의 개선사항들을 달성해가는 과정을 기술하였다. 우선 자성나노입자를 합성하여 코드화된 마이크로 입자에 포함시켜 입자를 다루기 쉽게 하였을 뿐 아니라 표면처리 과정에서 발생하는 입자간 차이를 줄였다. 또한 코드화된 마이크로 입자의 대량 양산 시스템을 구축하였고, 동시에 입자 생산

과정에서 발생하는 차이를 줄였다. 마지막으로 이 방법으로 생산한 마이크로 입자를 이용함으로써 개선된 다중화 어세이 결과를 보였다.

주요어: 다중화 어세이, 바이오 어세이, 코드화된 입자, 대량 양산, 자성나노입자, 초상자성

학번: 2011-20827